

Catalytic CO Oxidation by O₂ Mediated by Noble-Metal-Free Cluster Anions Cu₂VO₃₋₅⁻

Li-Na Wang, Xiao-Na Li,* Li-Xue Jiang, Bin Yang, Qing-Yu Liu, Hong-Guang Xu, Wei-Jun Zheng,* and Sheng-Gui He*

Abstract: Catalytic CO oxidation by molecular O₂ is an important model reaction in both the condensed phase and gas-phase studies. Available gas-phase studies indicate that noble metal is indispensable in catalytic CO oxidation by O₂ under thermal collision conditions. Herein, we identified the first example of noble-metal-free heteronuclear oxide cluster catalysts, the copper–vanadium bimetallic oxide clusters Cu₂VO₃₋₅⁻ for CO oxidation by O₂. The reactions were characterized by mass spectrometry, photoelectron spectroscopy, and density functional calculations. The dynamic nature of the Cu–Cu unit in terms of the electron storage and release is the driving force to promote CO oxidation and O₂ activation during the catalysis.

Catalytic carbon monoxide (CO) oxidation by molecular oxygen (O₂) is an important prototypical reaction in both condensed phase^[1] and gas-phase catalysis.^[2–4] Condensed-phase studies can develop catalysts that can be directly used for removal of poisonous CO, while gas-phase studies with state-of-the-art mass spectrometry in conjunction with quantum chemistry calculations can uncover the molecular- and electronic-level mechanisms that govern catalytic CO oxidation. It is noteworthy that the findings on catalytic CO oxidation (such as mechanisms of oxygen activation) from gas-phase studies can parallel well those from condensed-phase experiments.^[3a,b,5]

Available gas-phase experiments indicate that a noble metal (NM) is indispensable in catalytic CO oxidation by O₂

under thermal collision conditions,^[2,3] although many NM-free species can catalyze CO oxidation by N₂O.^[6] Two or more NM atoms are needed when the catalytic reaction (2CO + O₂ → 2CO₂) is mediated by bare or homonuclear metal oxide clusters, including Au₂⁻,^[2c,d] Au₆⁻,^[2b] Au₃(CO)₂₋₅,^[2f] Ag_n⁻ ($n = 7, 9, 11$),^[2e] Pt_nO_m⁻ ($n = 3–6$; $m = 0–2$),^[2a] and Pd₆O₃₋₅⁺.^[2g] Our recent studies revealed that single Au and Pt atoms doped heteronuclear oxide clusters AuAl₃O₃₋₅⁺^[3a] and PtAl₃O₅₋₇⁻^[3b] can catalyze CO oxidation by O₂. Notably, Ichihashi and co-workers reported the reactions of copper cluster anions with O₂ and CO and found that some clusters such as Cu₅O₂⁻ can catalyze CO oxidation at the collision energy of 0.2 eV.^[4k] The calculated reaction profile suggested that the reaction should also proceed under thermal collision conditions. Herein, we demonstrated unambiguously that the catalytic CO oxidation by O₂ can be mediated by copper–vanadium bimetallic oxide clusters Cu₂VO_m⁻ ($m = 3, 4$, and 5). Copper is a metal with low cost, high abundance, and potential use in a wide range of catalytic applications.^[7] Vanadium oxides are well-known catalysts and catalytic supports.^[8] This study serves as the first example of catalytic CO oxidation by O₂ on gas-phase heteronuclear oxide cluster catalysts without NM atoms.

The laser-ablation-generated Cu₂V¹⁸O₃₋₅⁻ clusters were mass-selected, confined, and thermalized through collisions with helium atoms, and then they were allowed to interact with CO, O₂, and a gas mixture of CO and O₂ in an ion trap reactor (see the Supporting Information).^[9] It should be noted that copper has two stable isotopes (69.15 % ⁶³Cu and 30.85 % ⁶⁵Cu) while the experiment was run to mass-select the ⁶³Cu₂ isotopomers. Figure 1 a,b,c shows the mass spectra of mass-selected Cu₂V¹⁸O_m⁻ clusters ($m = 5, 4$, and 3, respectively) when the reactor is only filled with inert bath gas (He). When the reactant gas CO, O₂, or CO + O₂ was injected into the reactor to interact with the mass-selected ions, new product ions could appear as shown in Figure 1 d–k (see the caption of Figure 1 for the experimental conditions).

Figure 1 d indicates that after interaction of CO with Cu₂VO₅⁻, two product ions Cu₂VO₄⁻ and Cu₂VO₃⁻ appear. CO can also react with Cu₂VO₄⁻ to give rise to products Cu₂VO₃⁻ and Cu₂VO₃CO⁻ (Figure 1 e). The Cu₂VO₃CO⁻ and Cu₂VO₃(CO)⁻ products appear after the reaction of CO with Cu₂VO₃⁻ (Figure 1 f). On the interactions of ¹⁶O₂ with the mass-selected clusters, the Cu₂V¹⁸O₃⁻ can pick up an ¹⁶O₂ to generate Cu₂V¹⁸O₃¹⁶O₂⁻ (Figure 1 i) while the Cu₂V¹⁸O₃⁻ is completely inert toward ¹⁶O₂ (Figure 1 g). A weak product peak Cu₂V¹⁸O₄¹⁶O₂⁻ was observed in the reaction of Cu₂V¹⁸O₄⁻ with ¹⁶O₂ (Figure 1 h). The primary reactions are listed below (see the Supporting Information for all of the reactions derived from Figure 1 a-i).

[*] L.-N. Wang, Dr. X.-N. Li, L.-X. Jiang, Dr. Q.-Y. Liu, Prof. S.-G. He
State Key Laboratory for Structural Chemistry of Unstable and Stable Species, Institute of Chemistry, Chinese Academy of Sciences
Beijing 100190 (China)

E-mail: lxn@iccas.ac.cn
shengguihe@iccas.ac.cn

B. Yang, Dr. H.-G. Xu, Prof. W.-J. Zheng
State Key Laboratory of Molecular Reaction Dynamics
Institute of Chemistry, Chinese Academy of Sciences
Beijing 100190 (China)

E-mail: zhengwj@iccas.ac.cn

L.-N. Wang, L.-X. Jiang, B. Yang, Prof. S.-G. He
University of Chinese Academy of Sciences
Beijing 100049 (China)

L.-N. Wang, Dr. X.-N. Li, L.-X. Jiang, B. Yang, Dr. Q.-Y. Liu,
Dr. H.-G. Xu, Prof. W.-J. Zheng, Prof. S.-G. He
Beijing National Laboratory for Molecular Sciences, CAS Research/
Education Center of Excellence in Molecular Sciences
Beijing 100190 (China)

Supporting information and the ORCID identification number(s) for
the author(s) of this article can be found under:
<https://doi.org/10.1002/anie.201712129>.

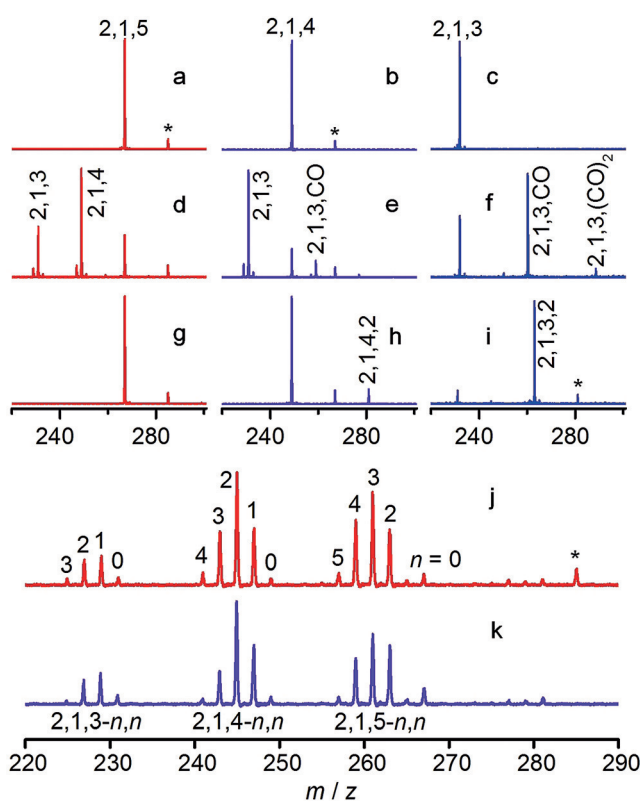


Figure 1. Mass spectra for elementary reactions of mass-selected $\text{Cu}_2\text{V}^{18}\text{O}_{3-5}^-$ clusters (a–c) with CO (d–f) and O_2 (g–i), and for catalytic reactions of mass-selected $\text{Cu}_2\text{V}^{18}\text{O}_5^-$ (j) and $\text{Cu}_2\text{V}^{18}\text{O}_4^-$ (k) with the gas mixture of C^{16}O and $^{16}\text{O}_2$. The CO partial pressures were 16 mPa (d), 24 mPa (e), and 144 mPa (f). The $^{16}\text{O}_2$ partial pressures were 396 mPa (g), 198 mPa (h), and 23 mPa (i). The gas mixture contains 74 mPa C^{16}O and 148 mPa $^{16}\text{O}_2$ for (j) and 50 mPa C^{16}O and 100 mPa $^{16}\text{O}_2$ for (k). The time periods for the reactions were 1.5 ms in (d)–(i) and 2.0 ms in (j) and (k). The $\text{Cu}_x\text{V}_y\text{O}_z^-$ and $\text{Cu}_x\text{V}_y\text{O}_z\text{CO}^-$ species are labeled as x,y,z and x,y,z,CO, respectively. $\text{Cu}_x\text{V}_y\text{O}_{z-n}{}^{16}\text{O}_n^-$ ($n \neq 0$) is labeled as x,y,z-n,n. Peaks marked with asterisks are due to water impurities.



The rate constants and reaction efficiencies for the above reactions have been determined and the results are summarized in Table 1. The elementary reactions (1), (2a), and (3a) can comprise a catalytic cycle for CO oxidation by molecular O_2 mediated with $\text{Cu}_2\text{VO}_{3-5}^-$ clusters.

To confirm the catalytic cycle, each of the $\text{Cu}_2\text{V}^{18}\text{O}_m^-$ ($m = 3, 4$, and 5) clusters was mass-selected and interacted with the gas mixture of C^{16}O and $^{16}\text{O}_2$ (Figure 1j,k; Supporting Information, Figures S4–S6). The experimental results indicated that the catalytic oxidation of CO by O_2 indeed takes place starting from any of the species $\text{Cu}_2\text{V}^{18}\text{O}_5^-$

Table 1: Reaction rate constants^[3a] and reaction efficiencies for the thermal reactions of $\text{Cu}_2\text{VO}_{3-5}^-$ with CO and O_2 .

Reaction	$k [10^{-10} \text{ cm}^3 \text{ molecule}^{-1} \text{ s}^{-1}]$	$\phi [\%]^{[a]}$
1	2.4 ± 0.8	34 ± 11
2a	2.2 ± 0.7	31 ± 10
2b	0.013 ± 0.004	0.21 ± 0.07
3a	3.6 ± 1.2	54 ± 18
3b	0.23 ± 0.08	3.2 ± 1.1

[a] $\phi = k/k_{\text{ADO}}, k_{\text{ADO}}$ is the theoretical collision rate.^[10]

(Figure 1j), $\text{Cu}_2\text{V}^{18}\text{O}_4^-$ (Figure 1k), and $\text{Cu}_2\text{V}^{18}\text{O}_3^-$ (Supporting Information, Figure S6). For example, the cluster source generated $\text{Cu}_2\text{V}^{18}\text{O}_5^-$ can oxidize two CO molecules to generate $\text{Cu}_2\text{V}^{18}\text{O}_4^-$ and $\text{Cu}_2\text{V}^{18}\text{O}_3^-$ (Reactions (1) and (2a)). The resulting $\text{Cu}_2\text{V}^{18}\text{O}_3^-$ can pick up one $^{16}\text{O}_2$ molecule to generate $\text{Cu}_2\text{V}^{18}\text{O}_3{}^{16}\text{O}_2^-$ (Reaction (3a)), and such formed $\text{Cu}_2\text{V}^{18}\text{O}_3{}^{16}\text{O}_2^-$ can then oxidize another two CO molecules, and so forth. Figure 1j indicates that starting from $\text{Cu}_2\text{V}^{18}\text{O}_5^-$, the ^{18}O atoms in $\text{Cu}_2\text{V}^{18}\text{O}_5^-$ can be substituted by isotopic ^{16}O to generate $\text{Cu}_2\text{V}^{18}\text{O}_3{}^{16}\text{O}_2^-$, $\text{Cu}_2\text{V}^{18}\text{O}_2{}^{16}\text{O}_3^-$, $\text{Cu}_2\text{V}^{18}\text{O}_3{}^{16}\text{O}_4^-$, and $\text{Cu}_2\text{V}^{16}\text{O}_5^-$. The generation of $\text{Cu}_2\text{V}^{18}\text{O}_{4-n}{}^{16}\text{O}_n^-$ ($n = 0$ –4) and $\text{Cu}_2\text{V}^{18}\text{O}_{3-n}{}^{16}\text{O}_n^-$ ($n = 0$ –3) further confirms the catalysis. The side reactions (2b) and (3b) observed in the elementary reactions (Figure 1e,f,h) barely appear in the catalytic reactions (Figure 1j,k). This result can be due to the difference of the effective cluster temperatures in the elementary versus the catalytic reactions.^[3a]

Density functional theory (DFT) calculations have been performed to explore the structures of $\text{Cu}_2\text{VO}_{3-5}^-$ clusters (Figure 2; Supporting Information, Figure S8) and the mechanisms of CO oxidation catalyzed by $\text{Cu}_2\text{VO}_{3-5}^-$ (Figure 3; Supporting Information, Figures S9–S12). The lowest-lying

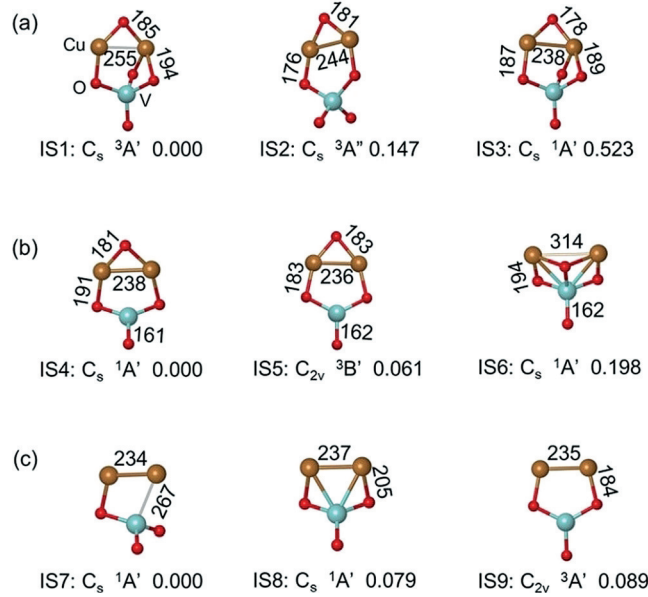


Figure 2: DFT-calculated low-lying isomers of Cu_2VO_5^- (a), Cu_2VO_4^- (b), and Cu_2VO_3^- (c). The bond lengths and relative energies are in units of pm and eV, respectively. Superscripts 1 and 3 denote the spin multiplicity.

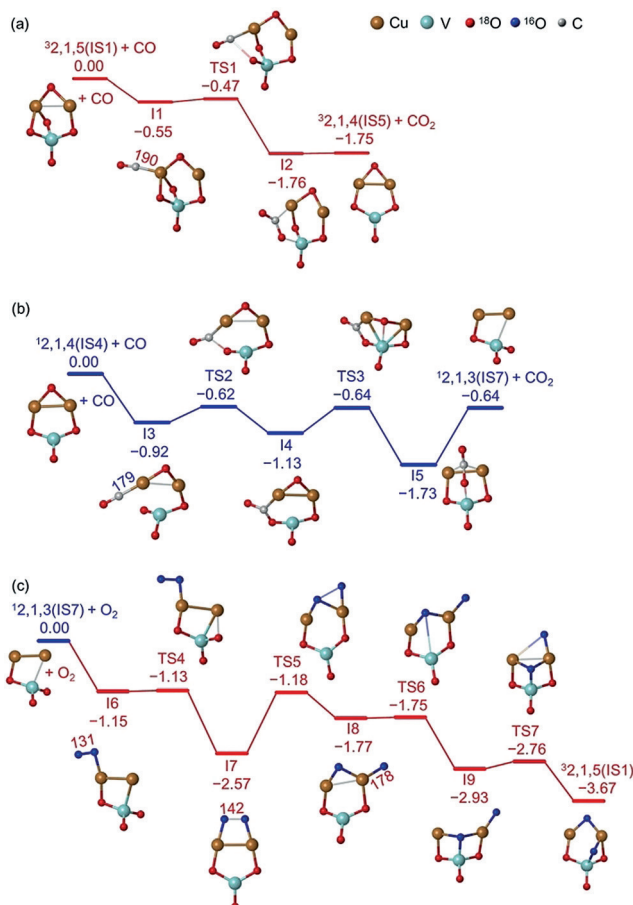


Figure 3. DFT-calculated potential energy profiles for reactions (1), (2a), and (3a). The bond lengths and relative energies are in units of pm and eV, respectively. ${}^M\text{Cu}_x\text{V}_y\text{O}_z^-$ is labeled as ${}^M_{x,y,z}$, and M denotes the spin multiplicity.

isomer of Cu_2VO_5^- (IS1, Figure 2) has a triplet spin state. The two unpaired electrons in IS1 are delocalized on two Cu atoms ($0.80 \mu_B$) and four surrounding oxygen atoms ($1.20 \mu_B$). In contrast, the lowest-lying isomers of Cu_2VO_4^- (IS4) and Cu_2VO_3^- (IS7) are in the singlet states (Figure 2). The structure and spin state of ${}^1\text{Cu}_2\text{VO}_4^-$ were further experimentally confirmed by photoelectron spectroscopy (Supporting Information, Figure S7).

As shown in Figure 3, the half-naked Cu atom in ${}^3\text{Cu}_2\text{VO}_5^-$ (IS1) can anchor CO with a binding energy of 0.55 eV (I1, Figure 3a). One of the two oxygen atoms bridging the Cu atom and the V atom can be abstracted to form a bent CO_2 unit (I1 \rightarrow TS1 \rightarrow I2) with a small barrier of 0.08 eV . In the next step, CO_2 desorption proceeds favorably to generate a triplet ${}^3\text{Cu}_2\text{VO}_4^-$ (IS5). Note that ${}^3\text{Cu}_2\text{VO}_5^-$ (IS1) can also oxidize CO to generate the singlet ${}^1\text{Cu}_2\text{VO}_4^-$ (IS4) favorably through a spin crossing^[11] from triplet to singlet spin state if CO approaches the other Cu atom (Supporting Information, Figure S10). Notably, the DFT method may not be accurate enough to determine the lowest-lying isomer in the experiment. Thus, the reactions of low-lying isomers of Cu_2VO_5^- (IS2 and IS3) with CO were also studied theoretically (Supporting Information, Fig-

ure S9). The calculated results indicated that both of the reactions ($\text{IS2} + \text{CO} \rightarrow \text{IS5} + \text{CO}_2$, $\text{IS3} + \text{CO} \rightarrow \text{IS4} + \text{CO}_2$) are favorable.

For the reaction of the singlet ${}^1\text{Cu}_2\text{VO}_4^-$ (IS4) with CO (Figure 3b), one of the oxygen atoms bridging the Cu atom and the V atom participates in CO oxidation in which the first step is subject to a barrier of 0.30 eV (I3 \rightarrow TS2 \rightarrow I4). Then desorption of a gas phase CO_2 to generate the singlet ${}^1\text{Cu}_2\text{VO}_3^-$ (IS7) is kinetically and thermodynamically favorable. Similarly, the other low-lying isomers of Cu_2VO_4^- (IS5 and IS6) can also oxidize CO to generate Cu_2VO_3^- (IS9 and IS7), as shown in the Supporting Information, Figure S11. After the consecutive CO oxidation, the Cu–Cu unit formed in the resulting Cu_2VO_3^- is of great importance to facilitate the attachment of O_2 and a large binding energy is released (I6 in Figure 3c, see also the Supporting Information, Figure S12). A negligible barrier of only 0.02 eV (I6 \rightarrow TS4 \rightarrow I7) is needed for further O_2 activation. The activation of O_2 can be well reflected by the significant elongation of the O–O bond, from 121 pm in free O_2 to 142 pm in I7. The subsequent formation of the initial ${}^3\text{Cu}_2\text{VO}_5^-$ (IS1) is calculated to be on a downhill pathway. The pathways on the reactions of Cu_2VO_3^- isomers (IS8 and IS9) with O_2 were also calculated (Supporting Information, Figure S12). The DFT calculations indicated that these low-lying isomers can also activate O_2 . The deviations by DFT for Cu–V–O system are in $\pm 0.3 \text{ eV}$ (Supporting Information, Table S1), while all of the calculated transition states are lower in energy than the separated reactants by more than 0.3 eV . Therefore, each of the elementary steps is barrierless overall. The computational results well support and interpret the experimental observations.

The activation and dissociation of molecular O_2 is generally highlighted as the rate determining step in catalytic CO oxidation.^[12] The Cu–Cu unit in Cu_2VO_3^- functions as the preferred trapping site to capture O_2 tightly (Figure 3c; Supporting Information, Figure S12). Natural bond orbital (NBO) analysis indicates that the Cu–Cu unit in Cu_2VO_3^- (IS7–IS9) is positively charged (Table 2). This property of

Table 2: Natural charges on the Cu–Cu units in low-lying isomers of $\text{Cu}_2\text{VO}_{3-5}^-$.

Cu_2VO_5^-	Q (e)	Cu_2VO_4^-	Q (e)	Cu_2VO_3^-	Q (e)
IS1	1.88	IS4	1.39	IS7	0.33
IS2	1.73	IS5	1.36	IS8	0.51
IS3	1.67	IS6	1.52	IS9	0.56

Cu_2VO_3^- is remarkably different from that of the oxygen deficient system Au_2TiO^- or Au_2VO_2^- that has two separate $\text{Au}^\delta-\text{M}^{\delta+}$ ($\text{M} = \text{Ti}$ or V) bonds and is completely inert toward molecular O_2 .^[5,13] The electronic feature of Cu is of great importance to facilitate the charge transfer interaction between the Cu–Cu unit and molecular O_2 . During O_2 adsorption, significant negative charge (-0.46 e in IS7, -0.76 e in IS8, and -0.71 e in IS9) is transferred dominantly from the Cu–Cu unit into the $2\pi^*$ orbital of O_2 and then the O_2 is significantly activated. This unique reactivity of

Cu_2VO_3^- toward molecular O_2 can be traced back to the multivalent nature of copper with Cu^0 , Cu^{1+} , Cu^{2+} , and even Cu^{3+} oxidation states,^[14] which facilitates formation of oxygen off-stoichiometry species. Thus, the copper oxides are greatly important in a wide range of chemical reactions involving the oxygen release and intake processes.^[14a, 15] These factors well rationalize the reactivity of Cu_2VO_3^- toward molecular O_2 .

The variation of NBO charges on the vanadium atom is small (Supporting Information, Table S2). However, the V atom plays a crucial role for the catalysis. The V atom is four and three-fold coordinated with O atoms in Cu_2VO_5^- and Cu_2VO_3^- , respectively (Figure 2). Thus, the V atom helps to store and release the O atoms ($\text{VO}_4 \leftrightarrow \text{VO}_3$). Note that none of the homo-nuclear Cu_2O_y^q species has been reported to catalyze CO oxidation by O_2 .^[4k,m,6n] Moreover, the negatively charged VO_3 moiety and the positively charged Cu–Cu unit in Cu_2VO_3^- results in a large dipole moment (8.84, 7.14, 7.25 D for IS7, IS8, IS9, respectively), which can polarize and activate O_2 during Reaction (3a).^[16]

Cu and Au are in the same group in the periodic table. The previous study indicates that single Au atom doped aluminum oxide clusters $\text{AuAl}_3\text{O}_{3.5}^+$ can catalyze CO oxidation by O_2 .^[3a] The charge cycling on the gold atom ($\text{Au}^+ \leftrightarrow \text{Au}^-$) drives the catalytic cycle. Herein, the Cu–Cu unit can also accept a significant amount of negative charge (Table 2) during consecutive CO oxidation ($\text{Cu}_2\text{VO}_5^- \rightarrow \text{Cu}_2\text{VO}_4^- \rightarrow \text{Cu}_2\text{VO}_3^-$) and the stored negative charge can be released during O_2 activation ($\text{Cu}_2\text{VO}_3^- \rightarrow \text{Cu}_2\text{VO}_5^-$), suggesting that the Cu₂ unit functions effectively as a single Au atom. The mechanism of O_2 activation by the Cu₂ dimer in this study parallels similar behavior of bioelectro-reduction of oxygen by multi-copper oxidoreductases (such as laccase)^[17] in which the dynamic nature of the Cu atoms in terms of electron cycling is the driving force to promote O_2 reduction.

In conclusion, we identified the first example of NM free heteronuclear oxide cluster catalysts to catalyze CO oxidation by O_2 . The oxidation catalysis is driven by electron cycling on Cu–Cu unit in $\text{Cu}_2\text{VO}_{3.5}^-$. For the crucial step of molecular O_2 activation, the well charge separation between the negatively charged VO_3 unit and the positively charged Cu–Cu unit in Cu_2VO_3^- greatly facilitates charge transfer interaction between the Cu–Cu unit and molecular O_2 . This gas-phase study provides the molecular-level insights into the nature of copper catalysis. The fundamental mechanisms behind the interesting results are helpful in the design of cost-effective heterogeneous catalysts as well as in the understanding of O_2 reduction by multi-copper oxidoreductases.

Acknowledgements

This work was financially supported by the National Natural Science Foundation of China (Nos. 21325314, 21773254, and 21573246), and the Beijing Natural Science Foundation (2172059). X.-N.L. thanks the grant from the Youth Innovation Promotion Association, Chinese Academy of Sciences (2016030).

Conflict of interest

The authors declare no conflict of interest.

Keywords: carbon monoxide · copper · heterogeneous catalysis · mass spectrometry · vanadium

How to cite: *Angew. Chem. Int. Ed.* **2018**, *57*, 3349–3353
Angew. Chem. **2018**, *130*, 3407–3411

- [1] a) H.-J. Freund, G. Meijer, M. Scheffler, R. Schlögl, M. Wolf, *Angew. Chem. Int. Ed.* **2011**, *50*, 10064–10094; *Angew. Chem.* **2011**, *123*, 10242–10275; b) S. Royer, D. Duprez, *ChemCatChem* **2011**, *3*, 24–65; c) B. Qiao, A. Wang, X. Yang, L. F. Allard, Z. Jiang, Y. Cui, J. Liu, J. Li, T. Zhang, *Nat. Chem.* **2011**, *3*, 634–641; d) A. Nilsson, J. LaRue, H. Öberg, H. Ogasawara, M. Dell’Angelica, M. Beye, H. Östrom, J. Gladh, J. K. Nørskov, W. Wurth, F. Abild-Pedersen, L. G. M. Pettersson, *Chem. Phys. Lett.* **2017**, *675*, 145–173.
- [2] a) Y. Shi, K. M. Ervin, *J. Chem. Phys.* **1998**, *108*, 1757–1760; b) W. T. Wallace, R. L. Whetten, *J. Am. Chem. Soc.* **2002**, *124*, 7499–7505; c) L. D. Socaciu, J. Hagen, T. M. Bernhardt, L. Wöste, U. Heiz, H. Häkkinen, U. Landman, *J. Am. Chem. Soc.* **2003**, *125*, 10437–10445; d) H. Häkkinen, U. Landman, *J. Am. Chem. Soc.* **2001**, *123*, 9704–9705; e) L. D. Socaciu, J. Hagen, J. Le Roux, D. Popolan, T. M. Bernhardt, L. Wöste, S. Vajda, *J. Chem. Phys.* **2004**, *120*, 2078–2081; f) Y. Xie, F. Dong, E. R. Bernstein, *Catal. Today* **2011**, *177*, 64–71; g) S. M. Lang, I. Fleischer, T. M. Bernhardt, R. N. Barnett, U. Landman, *J. Am. Chem. Soc.* **2012**, *134*, 20654–20659; h) S. M. Lang, I. Fleischer, T. M. Bernhardt, R. N. Barnett, U. Landman, *ACS Catal.* **2015**, *5*, 2275–2289.
- [3] a) Z.-Y. Li, Z. Yuan, X.-N. Li, X.-N. Li, S.-G. He, *J. Am. Chem. Soc.* **2014**, *136*, 14307–14313; b) X.-N. Li, Z. Yuan, J.-H. Meng, Z.-Y. Li, S.-G. He, *J. Phys. Chem. C* **2015**, *119*, 15414–15420; c) X.-N. Li, X.-P. Zhou, S.-G. He, *Chin. J. Catal.* **2017**, *38*, 1515–1527; d) H. Schwarz, *Catal. Sci. Technol.* **2017**, DOI: <https://doi.org/10.1039/C6CY02658C>.
- [4] a) M. K. Beyer, C. B. Berg, V. E. Bondybey, *Phys. Chem. Chem. Phys.* **2001**, *3*, 1840–1847; b) M. Brönstrup, D. Schröder, I. Kretzschmar, H. Schwarz, J. N. Harvey, *J. Am. Chem. Soc.* **2001**, *123*, 142–147; c) M. L. Kimble, A. W. Castleman, Jr., C. Bürgel, V. Bonačić-Koutecký, *Int. J. Mass Spectrom.* **2006**, *254*, 163–167; d) C. K. Siu, S. J. Reitmeier, I. Balteanu, V. E. Bondybey, M. K. Beyer, *Eur. Phys. J. D* **2007**, *43*, 189–192; e) N. M. Reilly, J. U. Reveles, G. E. Johnson, J. M. del Campo, S. N. Khanna, A. M. Köster, A. W. Castleman, Jr., *J. Phys. Chem. C* **2007**, *111*, 19086–19097; f) C. Bürgel, N. M. Reilly, G. E. Johnson, R. Mitić, M. L. Kimble, A. W. Castleman, Jr., V. Bonačić-Koutecký, *J. Am. Chem. Soc.* **2008**, *130*, 1694–1698; g) Y. Xie, F. Dong, S. Heinbuch, J. J. Rocca, E. R. Bernstein, *Phys. Chem. Chem. Phys.* **2010**, *12*, 947–959; h) D. M. Popolan, T. M. Bernhardt, *J. Chem. Phys.* **2011**, *134*, 091102; i) S. M. Lang, T. Schnabel, T. M. Bernhardt, *Phys. Chem. Chem. Phys.* **2012**, *14*, 9364–9370; j) Z.-C. Wang, S. Yin, E. R. Bernstein, *J. Phys. Chem. Lett.* **2012**, *3*, 2415–2419; k) S. Hirabayashi, Y. Kawazoe, M. Ichihashi, *Eur. Phys. J. D* **2013**, *67*, 1–6; l) K. Sakuma, K. Miyajima, F. Mafuné, *J. Phys. Chem. A* **2013**, *117*, 3260–3265; m) S. Hirabayashi, M. Ichihashi, Y. Kawazoe, T. Kondow, *J. Phys. Chem. A* **2012**, *116*, 8799–8806.
- [5] L.-N. Wang, Z.-Y. Li, Q.-Y. Liu, J.-H. Meng, S.-G. He, T.-M. Ma, *Angew. Chem. Int. Ed.* **2015**, *54*, 11720–11724; *Angew. Chem.* **2015**, *127*, 11886–11890.
- [6] a) M. M. Kappes, R. H. Staley, *J. Am. Chem. Soc.* **1981**, *103*, 1286–1289; b) D. K. Böhme, H. Schwarz, *Angew. Chem. Int. Ed.* **2005**, *44*, 2336–2354; *Angew. Chem.* **2005**, *117*, 2388–2406; c) V.

- Blagojevic, D. K. Böhme, *Int. J. Mass Spectrom.* **2006**, *254*, 152–154; d) V. Blagojevic, M. J. Y. Jarvis, E. Flaim, G. K. Koyanagi, V. V. Lavrov, D. K. Böhme, *Angew. Chem. Int. Ed.* **2003**, *42*, 4923–4927; *Angew. Chem.* **2003**, *115*, 5073–5077; e) V. Blagojevic, G. Orlova, D. K. Böhme, *J. Am. Chem. Soc.* **2005**, *127*, 3545–3555; f) G. E. Johnson, E. C. Tyo, A. W. Castleman, Jr., *J. Phys. Chem. A* **2008**, *112*, 4732–4735; g) E. C. Tyo, M. Nößler, R. Mitić, V. Bonačić-Koutecký, A. W. Castleman, Jr., *Phys. Chem. Chem. Phys.* **2011**, *13*, 4243–4249; h) Z.-C. Wang, N. Dietl, R. Kretschmer, T. Weiske, M. Schlangen, H. Schwarz, *Angew. Chem. Int. Ed.* **2011**, *50*, 12351–12354; *Angew. Chem.* **2011**, *123*, 12559–12562; i) Z. C. Wang, S. Yin, E. R. Bernstein, *Phys. Chem. Chem. Phys.* **2013**, *15*, 10429–10434; j) J. B. Ma, Z. C. Wang, M. Schlangen, S. G. He, H. Schwarz, *Angew. Chem. Int. Ed.* **2013**, *52*, 1226–1230; *Angew. Chem.* **2013**, *125*, 1264–1268; k) A. Yamada, K. Miyajima, F. Mafuné, *Phys. Chem. Chem. Phys.* **2012**, *14*, 4188–4195; l) O. P. Balaj, I. Balteanu, T. T. J. Roßteuscher, M. K. Beyer, V. E. Bondybey, *Angew. Chem. Int. Ed.* **2004**, *43*, 6519–6522; *Angew. Chem.* **2004**, *116*, 6681–6684; m) G. E. Johnson, R. Mitić, E. C. Tyo, V. Bonačić-Koutecký, A. W. Castleman, Jr., *J. Am. Chem. Soc.* **2008**, *130*, 13912–13920; n) S. Hirabayashi, M. Ichihashi, *Phys. Chem. Chem. Phys.* **2014**, *16*, 26500–26505; o) X. Sun, S. Zhou, L. Yue, M. Schlangen, H. Schwarz, *Angew. Chem. Int. Ed.* **2017**, *56*, 9990–9993; *Angew. Chem.* **2017**, *129*, 10122–10126.
- [7] R. Prasad, P. Singh, *Catal. Rev. Sci. Eng.* **2012**, *54*, 224–279.
- [8] G. Ertl, H. Knözinger, J. Weitkamp, *Handbook of Heterogeneous Catalysis*, Wiley-VCH, New York, **1997**.
- [9] Z. Yuan, Z.-Y. Li, Z.-X. Zhou, Q.-Y. Liu, Y.-X. Zhao, S.-G. He, *J. Phys. Chem. C* **2014**, *118*, 14967–14976.
- [10] G. Kummerlöwe, M. K. Beyer, *Int. J. Mass Spectrom.* **2005**, *244*, 84–90.
- [11] a) D. Schröder, S. Shaik, H. Schwarz, *Acc. Chem. Res.* **2000**, *33*, 139–145; b) J. N. Harvey, *Phys. Chem. Chem. Phys.* **2007**, *9*, 331–343.
- [12] a) G. I. Panov, K. A. Dubkov, E. V. Starokon, *Catal. Today* **2006**, *117*, 148–155; b) A. P. Woodham, G. Meijer, A. Fielicke, *Angew. Chem. Int. Ed.* **2012**, *51*, 4444–4447; *Angew. Chem.* **2012**, *124*, 4520–4523; c) A. P. Woodham, G. Meijer, A. Fielicke, *J. Am. Chem. Soc.* **2013**, *135*, 1727–1730; d) J. Hagen, L. D. Socaciu, J. Le Roux, D. Popolan, T. M. Bernhardt, L. Wöste, R. Mitić, H. Noack, V. Bonačić-Koutecký, *J. Am. Chem. Soc.* **2004**, *126*, 3442–3443; e) B. E. Salisbury, W. T. Wallace, R. L. Whetten, *Chem. Phys.* **2000**, *262*, 131–141; f) R. Pal, L.-M. Wang, Y. Pei, L.-S. Wang, X.-C. Zeng, *J. Am. Chem. Soc.* **2012**, *134*, 9438–9445; g) W. Huang, H.-J. Zhai, L.-S. Wang, *J. Am. Chem. Soc.* **2010**, *132*, 4344–4351; h) Z.-P. Liu, X.-Q. Gong, J. Kohanoff, C. Sanchez, P. Hu, *Phys. Rev. Lett.* **2003**, *91*, 266102; i) Y. D. Kim, M. Fischer, G. Ganteför, *Chem. Phys. Lett.* **2003**, *377*, 170–176; j) U. Heiz, A. Sanchez, S. Abbet, W. D. Schneider, *J. Am. Chem. Soc.* **1999**, *121*, 3214–3217; k) B. Yoon, H. Häkkinen, U. Landman, A. S. Wörz, J. M. Antonietti, S. Abbet, K. Judai, U. Heiz, *Science* **2005**, *307*, 403–407.
- [13] X.-N. Li, Z.-Y. Li, H.-F. Li, S.-G. He, *Chem. Eur. J.* **2016**, *22*, 9024–9029.
- [14] a) J. S. Elias, N. Artrith, M. Bugnet, L. Giordano, G. A. Botton, A. M. Kolpak, Y. Shao-Horn, *ACS Catal.* **2016**, *6*, 1675–1679; b) F. Wang, R. Büchel, A. Savitsky, M. Zalibera, D. Widmann, S. E. Pratsinis, W. Lubitz, F. Schüth, *ACS Catal.* **2016**, *6*, 3520–3530.
- [15] L. Luo, L. Zhang, Z. Duan, A. S. Lapp, G. Henkelman, R. M. Crooks, *ACS Nano* **2016**, *10*, 8760–8769.
- [16] Y. Byun, W. S. Jeon, T.-W. Lee, Y.-Y. Lyu, S. Chang, O. Kwon, E. Han, H. Kim, M. Kim, H.-J. Lee, R. R. Das, *Dalton Trans.* **2008**, 4732–4741.
- [17] K. Piontek, M. Antorini, T. Choinowski, *J. Biol. Chem.* **2002**, *277*, 37663–37669.

Manuscript received: November 26, 2017

Revised manuscript received: January 25, 2018

Accepted manuscript online: January 28, 2018

Version of record online: February 21, 2018